2016 SNMMI Highlights Lecture: Oncology, Part 2

Wolfgang A. Weber, MD, Memorial Sloan–Kettering Cancer Center, New York, NY

From the Newsline Editor: The Highlights Lecture, presented at the closing session of each SNMMI Annual Meeting, was originated and presented for more than 30 years by Henry N. Wagner, Jr., MD. Beginning in 2010, the duties of summarizing selected significant presentations at the meeting were divided annually among 4 distinguished nuclear and molecular medicine subject matter experts. Each year Newsline publishes these lectures and selected images. The 2016 Highlights Lectures were delivered on June 15 at the SNMMI Annual Meeting in San Diego, CA. In this issue we feature part 2 of the lecture by Wolfgang A. Weber, MD, from the Memorial Sloan–Kettering Cancer Center (New York, NY), who spoke on highlights in oncology. The first part was published in the January issue of Newsline. Note that in the following presentation summary, numerals in brackets represent abstract numbers as published in The Journal of Nuclear Medicine *(2016;57[suppl 2]).*

Preclinical studies in nuclear therapy for cancer were an outstanding feature of this year's meeting. Yoshii and colleagues from the National Institute of Radiological Sciences (Chiba, Japan), Kawasaki Medical School (Kurashiki, Japan), National Cancer Center Hospital East (Chiba, Japan), and Research Centre Nihon Medi-Physics Co., Ltd. (Chiba, Japan) reported on "^{64}Cu-ATSM internal radiotherapy to treat colon cancer acquiring resistance to antiangiogenic therapy with bevacizumab" [471]. This was an elegant study that looked at a combination treatment with the antiangiogenic agent bevacizumab and ^{64}Cu-ATSM, which is taken up by hypoxic cells. ^{64}Cu can be used for both imaging and treatment, because the positrons and betas it emits can also be used as therapy. These investigators explored the hypothesis that during treatment with bevacizumab, blood flow would be decreased and hypoxia would be correspondingly increased, thereby making the tumor more resistant. At the same time, this process might make the tumor more sensitive to therapies that specifically target hypoxic cells. In experimental studies they showed that although the angiogenesis inhibitor bevacizumab alone had some effect on tumor growth, the therapeutic effect could be increased by combining this with the ^{64}Cu-ATSM agent. The hypoxia agent alone had no effect on treatment (Fig. 1). This confirmed their hypothesis that hypoxia can be induced and then treated with an additional drug and that this process can be imaged with SPECT/CT and PET/CT.

We are also seeing progress in the area of pretargeting. Cheal et al. from Memorial Sloan–Kettering Cancer Center (New York, NY) and the Massachusetts Institute of Technology (Cambridge, MA) reported on "Curative theranostic pretargeted radioimmunotherapy of GPA33-expressing colorectal cancer using a bispecific antibody with high affinity for GPA33 and DOTA metal complex (DPRIT)" [33]. This antibody has binding sites for GPA33, a cell surface protein overexpressed in colorectal cancer, and also for the complex of the chelator DOTA with several lanthanoids, such as yttrium and lutetium. The result is an antibody that can accumulate in tumor tissue over a period of several days if necessary, followed by injection of the DOTA, which is radiolabeled with either ^{177}Lu or ^{86}Y. The radiolabeled DOTA is cleared rapidly from the kidney and does not enter the intracellular space, so that radiation exposure of the normal tissue is minimal. These initial studies with this new pretargeting concept are very promising. After injecting the ^{177}Lu-DOTA antibody, a complete response was achieved in 10 out of 10 animals with colorectal cancer grafts, whereas untreated animals showed very rapid tumor growth (Fig. 2). This new pretargeting approach could therefore lead to novel applications of radioimmunotherapy with much less risk of hematologic toxicity than immunotherapy with radiolabeled antibodies.

Wolfgang A. Weber, MD

Expanding the Focus of ^{18}F-FDG PET

Although many studies presented at the SNMMI 2016 meeting looked at tracers other than FDG, even more studies continued to focus on FDG, which at this meeting was called "the molecule of the century." But I would like to pose a question: what *is* an FDG PET/CT image? We often think of the SUV_{max} quantified from a single voxel as representing everything we want to know about a PET/CT. But as is clear, the PET/CT image is much more complex. At the meeting a number of presentations offered new algorithms and novel computer approaches to capture the full range of information inherent in these images—not only the PET data but also the CT data—and then correlate these with patient outcomes. So many abstracts were presented in this category that I had to make difficult choices and picked only 2 to illustrate general principles. I offer my apologies to all of the investigators whose work could not be covered here.

Desseroit et al. from the Centres Hospitaliers Universitaires de Poitiers, Laboratoire de Traitement de l'Information Médicale UMR (Nantes), and Institut National de la Santé et de la Recherche Médicale Laboratoire de Traitement de l'Information Médicale UMR (Brest, France) reported on a "Nomogram for non–small cell lung cancer (NSCLC) exploiting clinical staging, tumor volume, and PET/CT heterogeneity features: development using support vector machines in a retrospective cohort and first validation results in prospectively recruited patients" [437]. This group looked

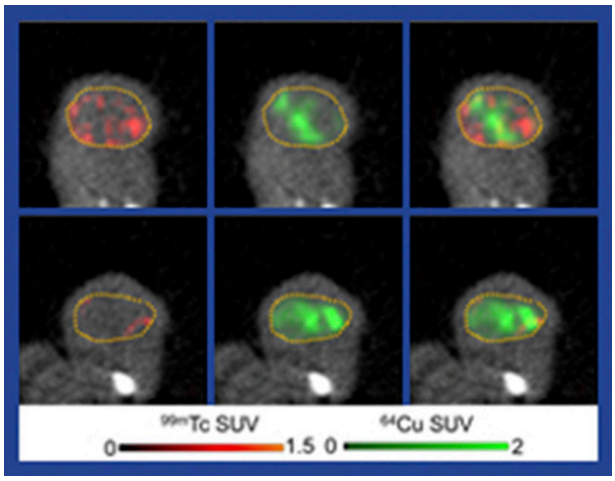

FIGURE 1. Characterization of bevacizumab-resistant tumors. SPECT/CT and PET/CT imaging with ^{99m}Tc-human serum albumin (left, blood pool) and ^{64}Cu-ATSM (middle, hypoxia). Right: fused images. Top: controls. Bottom: Bevacizumab-resistant tumor (after 3 weeks of bevacizumab treatment). Bevacizumab-resistant HT-29 tumors showed reduction of vascularity and increased hypoxic areas. The authors went on to study in vivo treatment with ^{64}Cu-ATSM + bevacizumab to target tumor angiogenesis and the induced hypoxia. The combination showed synergistic inhibition of tumor growth with minimal side effects.

at texture patterns in NSCLC and correlated these with patient outcomes, using the results to construct a predictive tool. Their interesting observation was that although (as expected) tumor stage as conventionally defined by the World Health Organization was correlated with patient outcomes, these texture features were significantly better correlated with patient outcomes. Intratumoral heterogeneity quantified with textural features in both CT and FDG PET images from routine PET/CT acquisitions was found to have complementary prognostic value to conventional staging in NSCLC. The nomogram, which combined information from clinical staging and tumor volume with texture analysis, resulted in identification of a specific tumor profile with very poor prognosis. One of the main reasons we perform staging is to predict patient outcome, so it is quite significant that we now may have a PET-based imaging test that might be better than analysis of resected tumor tissue or other imaging modalities in identifying patient outcomes.

Similar results were reported by Chan et al. from Chang-Gung Memorial Hospital (Taoyuan, Taiwan) with "Combination of ^{18}F-FDG PET/CT texture features with dynamic contrast-enhanced and diffusion-weighted MRI parameters for the prediction of prognosis in patients with primary oropharyngeal or hypopharyngeal squamous cell carcinoma" [1581]. The main finding of the study was that although tumor stage was somewhat correlated with patient outcome, analysis of tumor heterogeneity was significantly better correlated with patient outcomes. The authors concluded that ^{18}F-FDG PET/CT texture features appeared to be independent prognosticators of survival in patients treated with chemoradiation for oro- and hypopharyngeal squamous cell carcinoma. The combination of these PET texture features and MR parameters allowed improved prognostic stratification of patients. One risk of these types of complex analyses is that with sufficient numbers of parameters nice correlations may sometimes be identified that have little clinical relevance. But this approach certainly holds great promise and potential. I hope that next year we will have more prospective validation of the patterns described at this meeting to see whether these very strong correlations and predictions of patient outcomes hold true.

Tumor burden as assessed on PET imaging was also a focus of presenters this year. Again, time restrictions allow only 2 examples from the many studies presented in this area. Some critics might look at the topic of tumor burden as either obvious or trivial: we know that high tumor burden is associated with worse outcomes than lesser tumor burden. Although that is true, the important point that many of these presentations emphasized is that it is not enough to identify "better" or "worse"—we want to develop new methods for precisely identifying and describing tumor burden and correlating the resulting analyses with outcomes. An ^{18}F-FDG PET scan allows us to do this in many diseases in a highly automated fashion, something that is challenging with other imaging modalities. It is quite difficult to calculate total tumor burden from a CT scan, because, at least with current technology, manual delineation of many regions is required. With PET, however, simple thresholding approaches can define and quantify metabolic tumor volume. Cottereau, from Henri Mondor Hospital Creteil (France), and colleagues from Centre Henri Becquerel (Saint Aubin Épinay, France), Centre Hospitalier Lyon Sud (France), University of Sydney (Australia), Santa Maria Nuova Hospital (Reggio Emilia, Italy), and the University of Modena and Reggio Emilia (Modena, Italy) reported that "Baseline metabolic tumor volume predicts outcome in patients with high tumor burden follicular lymphoma" [30]. Another study from Uchiyama et al. from the Hokkaido University Graduate School of Medicine (Sapporo, Japan) reported that "Metabolic tumor volume and total lesion glycolysis on FDG PET are strong predictors for survival of patients with differentiated thyroid carcinoma—a comparison with SUV_{max}" [574]. Both these studies, in different diseases, found similar outcomes,

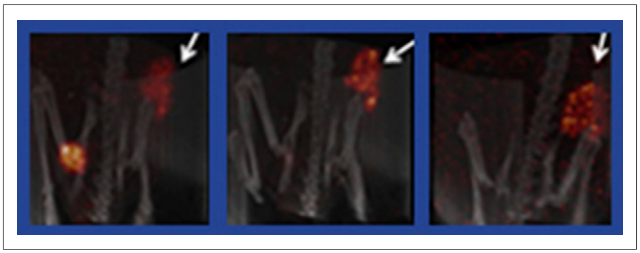

FIGURE 2. Serial noninvasive nanoSPECT/CT of mouse bearing colorectal cancer grafts undergoing DOTA metal complex treatment (55 MBq/cycle) at baseline (left) and 24 (middle) and 160 hours (right) after first-cycle ^{177}Lu-DOTA-Bn injection. Serial imaging was used for dosimetry calculations.

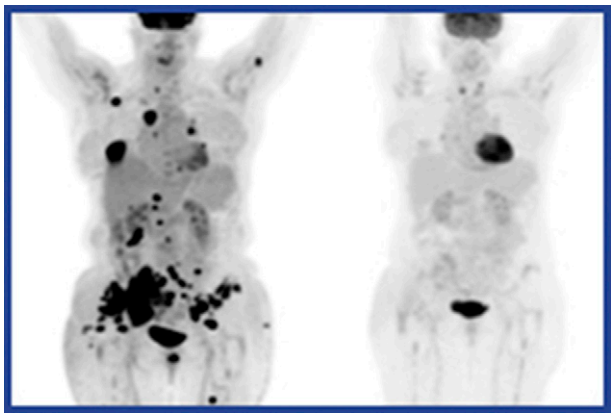

FIGURE 3. Example ^{18}F-FDG PET images of patient with non–small cell lung cancer treated with the PD-L1 inhibitor atezolizumab at baseline (left) and at week 6 after initiation of treatment (right). Patients in the study with metabolic response by European Organisation for Research and Treatment of Cancer criteria at week 6 had higher overall response rates by RECIST 1.1 than metabolic nonresponders (74% and 7%, respectively).

with extremely strong predictive values for metabolic tumor volume on PET imaging. These studies, if confirmed and prospectively validated, suggest that PET-assessed tumor volume should become an integral part of the staging system. In addition to benefiting clinical care, this metric should also be included in clinical trials. Research studies that include patients with different metabolic tumor volumes in different treatment arms might be inherently biased.

Imaging Cancer Immunotherapy

Cancer immunotherapy continues to be a focus in our field and others and has been called a major medical breakthrough of the last decade in extensive media coverage. A persistent problem, however, is that although some patients experience extraordinary benefits with immunotherapy, including long-term responses, others do not and progress very quickly. The challenge is to identify and validate ways to differentiate responders from nonresponders early in the course of treatment. ^{18}F-FDG PET has been investigated for this purpose by several groups. Mena et al. from the Johns Hopkins University (Baltimore, MD) reported on the "Predictive value of early ^{18}F-FDG PET/CT imaging for immunotherapy response assessment in metastatic melanoma patients" [408]. These researchers reported that early FDG PET imaging during immunotherapy either under- or overestimated response and that the predictive value of PET for patient outcome became significantly better at later stages.

Different perspectives were reported by other groups. Fredrickson et al. from Genentech (South San Francisco, CA), Memorial Sloan–Kettering Cancer Center (New York, NY), and Peter MacCallum Cancer Institute (East Melbourne, Australia) reported on the "Utility of FDG-PET in immunotherapy: results from a phase II study of NSCLC patients undergoing therapy with the PD-L1 inhibitor, atezolizumab (MPDL3280A)" [134]. In this study, the responders showed dramatic responses to treatment on FDG PET early (at 6 weeks) (Fig. 3), with no indication of a flare phenomenon. The utility of early PET in this setting appeared to be similar to that reported with conventional chemotherapeutic treatments, with early metabolic response predicting subsequent benefit. Baseline whole-body metabolic tumor volume was a strong negative predictor of overall survival. This certainly merits further study. Results may differ depending not only on the exact type of immunotherapy being investigated but also the tumor being studied. Much work remains to be done to explore FDG assessment of tumor response to these new immunotherapies.

Immunotherapies also provide opportunities for development of new imaging agents with which we may not only assess response but predict which patients will benefit from specific treatments. McQuade and colleagues from Merck & Co., Inc. (Palo Alto, CA, and West Point, PA) reported on "Investigation into use of PET as an in vivo imaging tool to quantify PD-L1 tumor expression levels" [529]. Programmed death-ligand 1 (PD-L1) is a transmembrane protein and immune regulatory ligand that is expressed on cancer cells and inhibits the immune response of the body to these cells. These investigators used ^{64}Cu to radiolabel an antihuman PD-L1 monoclonal antibody and tested it in mice. PET imaging showed that this antibody accumulated in human tumors

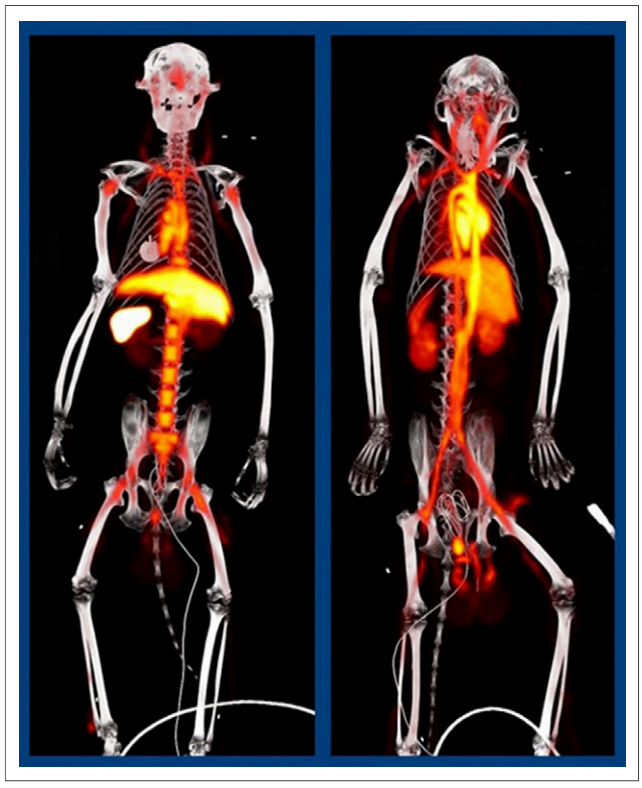

FIGURE 4. PET biodistribution imaging of the PD-L1–targeting ligand in healthy rhesus monkeys. Images with ^{64}Cu-DOTA-22C3 (left) and ^{64}Cu-DOTA-27F11 isotype matched control (right) acquired 3–3.5 hours after injection. Significantly higher spleen uptake and faster blood clearance were observed with ^{64}Cu-DOTA-22C3.

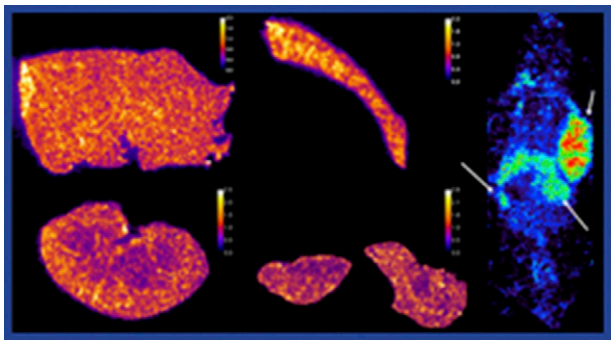

FIGURE 5. PD-L1 as a therapeutic target. Alpha-camera images (left and middle) acquired at 6 hours after injection showed that the majority of ^{225}Ac-anti-PD-L1 was located within the pelvis region of the kidneys, with a small uptake in medially situated proximal tubules in immunocompetent C57BL/6 mice. The scale shows relative activity distribution within the tissue sample to the average of the whole tissue sample, indicating 2.2–2.6 times higher activity in some areas of tissue than in the average of the whole tissue. SPECT image (right) at 24 hours after injection of ^{111}In-DTPA anti-PD-L1 24 and 48 hours after injection with a 3.0 mg/kg protein concentration showing higher uptake in tumor and less in spleen and liver.

transplanted in mice and that tumor could clearly be delineated from surrounding tissue. One issue with these and similar promising studies is that these PD-L1 antibodies are specific for human PD-L1; they do not bind to mouse PD-L1. The result is the potential for overestimating potential benefits based solely on preclinical studies, because there is no competition with the natural sink of the antibody that could also bind it in humans. The Merck investigators, however, went a step further and studied this PET ligand in rhesus monkeys. They showed binding to the PD-L1 not only in the spleen, where PD-L1 is expressed by lymphocytes and binding would be expected, but also in bone marrow. Other biodistribution appeared favorable (Fig. 4). The authors concluded that their results in tumor-bearing mice and in healthy

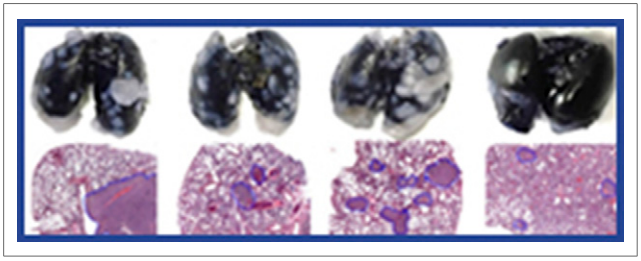

FIGURE 6. Initial local integrin αvβ6-targeted photodynamic therapy (PDT) promoted maturation of dendritic cells. When followed by PD-1 blocking, this treatment increased infiltration of CD8$^+$ T lymphocytes and inhibited growth of metastases in the lungs. Lungs of mice are stained in black, and metastases are visible as white nodules (top). Gross tumor (top) corresponding tissue sections (bottom) from (left to right) control mice, PDT alone, anti-PD-1 alone, and combined PDT and anti-PD-1.

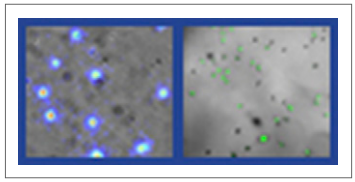

FIGURE 7. Radioluminescence microscopy of ^{18}F-fluorothymidine uptake (left) in live human MDA-MB-231 cells and, as a reference, uptake of 5-ethynyl-2′-deoxyuridine (EdU; right) in fixed cells. When FLT and EdU signal was quantified from cells, a clear distinction could be made between arrested and proliferating cells.

rhesus monkeys lend support to the hypothesis that PD-L1 may ultimately be imaged in vivo in the clinic using PET.

PD-L1 could also become a therapeutic target. Josefsson et al. from the Johns Hopkins University School of Medicine (Baltimore, MD) reported on "Dosimetric analysis of actinium-225 labeled anti-PD-L1 alpha particle radioimmunotherapy of melanoma cancer in an immunocompetent mouse model" [635]. In preliminary biodistribution studies they showed accumulation in the tumor and also significant uptake in the spleen. They were able to decrease the spleen uptake by changing the specific activity concentration of the antibody injected. Their biodistribution data and the results of early α-camera and SPECT imaging indicate that this may provide a useful therapeutic target (Fig. 5).

In reviewing therapy presentations at this meeting, I should also emphasize that several abstracts did not focus on radionuclides but, instead, on photodynamic therapy. Gao et al. from Peking University (Beijing, China) reported on

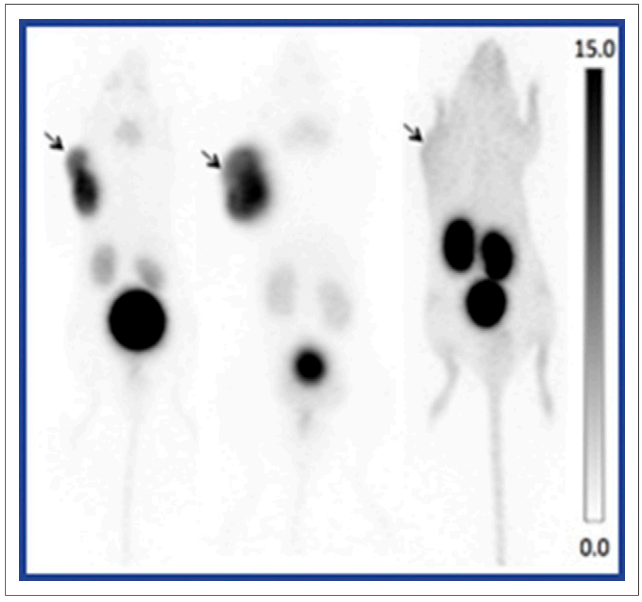

FIGURE 8. Targeting the melanocortin-1 receptor (MC1R) for PET melanoma imaging. The ^{68}Ga-CCZ01048 tracer, 1 of 3 assessed, had high binding affinity to MC1R and high in vivo stability. Addition of a cationic linker resulted in sustained tumor accumulation and fast clearance in normal tissues. Example images at 1 and 2 hours after injection and at 1 hour after injection of a blocking dose in C57BL/6J mice bearing B16-F10 tumors.

"Anti-tumor efficacy of combination integrin αvβ6-targeted photodynamic therapy and immune checkpoint inhibition" [85]. In this elegant study, the authors performed αvβ6-targeted photodynamic therapy on the primary tumor in a mouse model and then investigated how this treatment, in combination with an anti-PD1 inhibitor, affected formation of disease in other parts of the body. In theory, the initial treatment releases antigens that then stimulate the immune system to target tumors at other sites. The researchers not only proved this theory in their mouse model (Fig. 6) but also found that local photodynamic therapy improved survival and decreased the formation of lung metastases. At least in some animal models, then, we have evidence that local therapies can stimulate an immune response that then becomes effective for systemic disease.

A Growing Range of Topics

Although I have tried to group these highlights into several topical themes, many outstanding presentations did not fit neatly into these categories. Among these was the updated report of Sengupta and Pratx from Stanford University (CA) on "Radioluminescence microscopy of ^{18}F-fluorothymidine (^{18}F-FLT) uptake in single cells" [364]. This technology is fascinating, because it allows us to study the accumulation of radiotracers at the cellular level. Single cells can be analyzed under the microscope to measure uptake and analyze the distribution of tracer in cells of different phases. In this case, the authors characterized the single-cell distribution of ^{18}F-FLT and compared it against a standard fluorescence-based measure of cell proliferation (5-ethynyl-2′-deoxyuridine uptake). If we take tumor heterogeneity seriously and want to understand its effects on uptake in imaging and with specific agents, then this type of study is especially important. We need these microscopic techniques that will allow us to study the heterogeneity of targeting tracer uptake with high spatial resolution (Fig. 7).

Other targets were also investigated and presented at this meeting. Zhang et al. from British Columbia Cancer Research Centre (Vancouver) reported promising data on "Melanoma

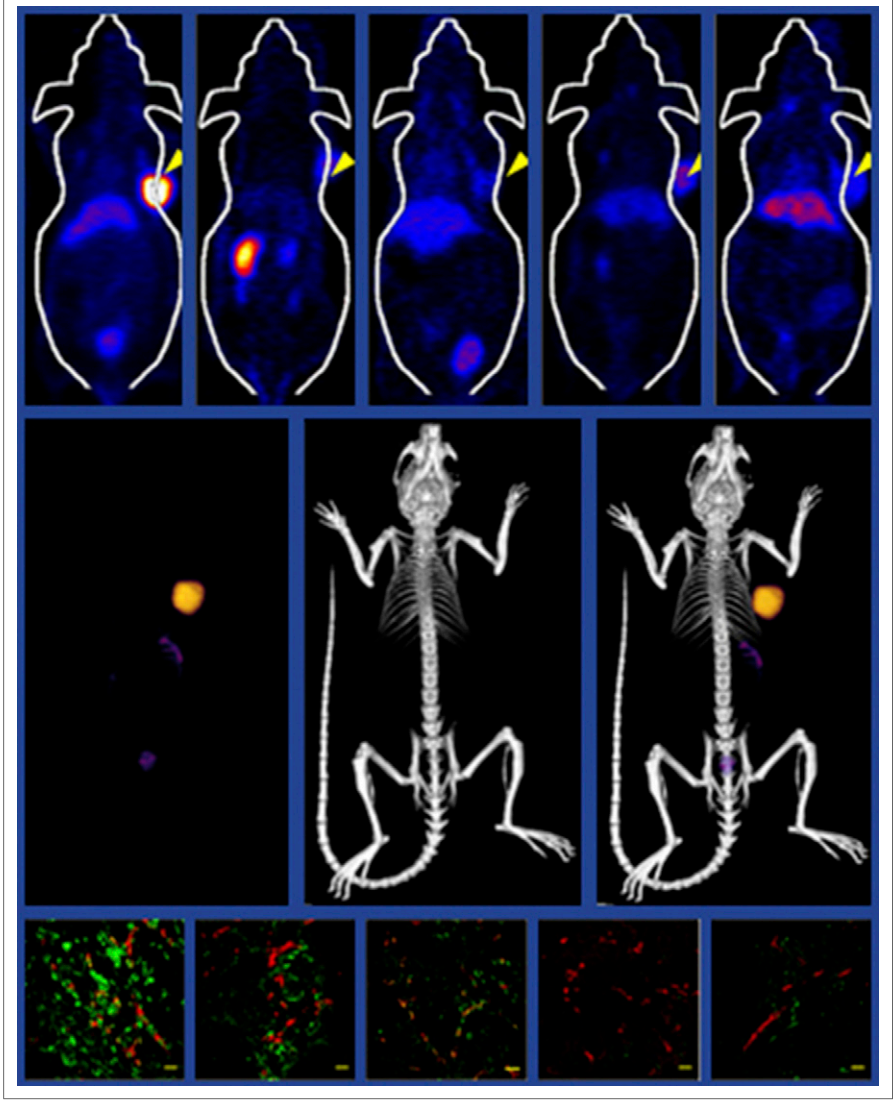

FIGURE 9. Dual-targeting using a heterodimer tracer offered a significant advantage in terms of absolute tumor uptake, target specificity, and off-target uptake, compared to monospecific Fab fragments. Top row: Coronal PET imaging in in vivo at 30 hours with (left to right) ^{64}Cu-NOTA-heterdimer, TF blocking, CD105 blocking, ^{64}Cu-NOTA-ALT-836-Fab, and ^{64}Cu-NOTA-TRC105-Fab. Middle row: PET (left), CT (middle), and PET/CT (right) with ^{64}Cu-NOTA-herodimer. Bottom row: immunofluorescence staining of ^{64}Cu-NOTA-heterodimer, ^{64}Cu-NOTA-836-Fab, ^{64}Cu-NOTA-TRC105-Fab, TF blocking, and CD105 blocking. In agreement with its TF/CD105 bivalent property, ^{64}Cu-NOTA-heterodimer staining showed a stronger fluorescent signal that distributed in both BXPC-3 cells and tumor-associated vasculature in the tissue. Blocking with ALT-836 or TRC105 resulted in low-intensity signals of TF/CD105 staining, confirming the TF/CD105 bispecificity of ^{64}Cu-NOTA-heterodimer. Green = TF/CD105; red = CD31.

imaging with ^{68}Ga-labeled cyclized α-melanocyte stimulating hormone peptides using PET" [3]. (Fig. 8). The authors found excellent tumor visualization and exceptional contrast with all 3 radiopeptides targeting the melanocortin-1 receptor for melanoma imaging. The use of a cationic linker led to high and sustained tumor uptake, excellent image contrast, and lower kidney accumulation in a mouse model. These results are promising for future applications in humans.

Progress is also being made in the complex area of dual targeting, which has long been the focus of investigations to both increase radiotracer uptake and elucidate different aspects of disease progression. Development in this area has proven more challenging than was initially anticipated. Luo et al. from the University of Wisconsin Madison reported on "Dual targeting of tissue factor (TF) and CD105 for PET imaging of pancreatic cancer" [51]. These researchers showed convincing evidence for the benefits of simultaneous antibody targeting of TF and CD105 for potential imaging and therapy of pancreatic cancer, in an approach that may effectively address current therapeutic limitations (Fig. 9). One interesting observation in this study is that although the monomer against TF and the monomer against CD105 showed only moderate uptake, the antibody that bound to both showed much higher uptake. The result is a synergistic effect in which dual targeting boosted uptake dramatically. At the same time, biodistribution in normal tissues was not correspondingly affected.

The last new tracer I would like to highlight is a tumor probe that allows the study of exosomes. Exosomes are tumor microvesicles containing RNA and DNA that are believed to play an important role in cell communication and also in the spread of tumor cells to the bone marrow and other organs. The ability to label those exosomes, follow them, and explore their physiologic function in vivo not only expands our knowledge of tumorigenesis but opens the interesting possibility of using exosomes as molecular probes. Nikolopoulou et al. from the Spanish National Cancer Research Center (Madrid, Spain), University of Nebraska (Lincoln), and Weill Cornell Medicine (New York, NY) reported on "Tumor exosomes as molecular probes to detect breast cancer premetastatic niches: radiolabeling with ^{131}I and tissue uptake studies in 'naïve' nude mice" [524]. These researchers radiolabeled the exosomes using standard techniques and showed that they remained functional, as indicated by uptake in cancer cells and in fibroblasts (Fig. 10). Biodistribution of these ^{131}I-exosomes could be followed over time in mice. The authors concluded that these findings suggest that radiolabeled exosomes can be used to determine the specificity and dynamics of distribution in vivo and help to define their role in tumor progression and premetastatic niche formation. Although this work is still in its early stages, it is exciting that we now have the potential to study and better understand the function of exosomes in tumor biology.

New tracers are being introduced into human studies, and I was very much impressed by the report from Chen et al. from the University of Pennsylvania (Philadelphia) and Washington University School of Medicine (St. Louis, MO) on "First-in-human studies characterizing a poly(ADP-ribose)polymerase (PARP) targeted tracer, ^{18}F-FluorThanatrace (^{18}F-FTT), for cancer imaging" [582]. PARP is an intracellular enzyme involved in DNA repair. Many imaging agents for intracellular targets have shown poor biodistribution with very unfavorable uptake and high background. But this imaging agent seems to have very clear biodistribution at 30 minutes postinjection and persisting at 120 min. As expected, uptake was seen in the spleen, where B lymphocytes express PARP. This group also presented some very preliminary data on tumor uptake in recurrent pancreatic cancer and in liver metastases in colon cancer (Fig. 11). This appears to be a very promising imaging agent to study the role of PARP in cancer and also to monitor PARP inhibitor therapy, which is currently being investigated in several malignancies.

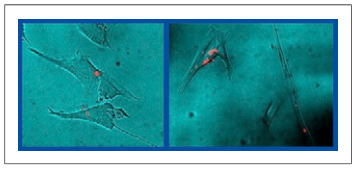

FIGURE 10. Fluorescent microscopy imaging of exosomes (red) at 24 hours in WI-38 lung fibroblasts.

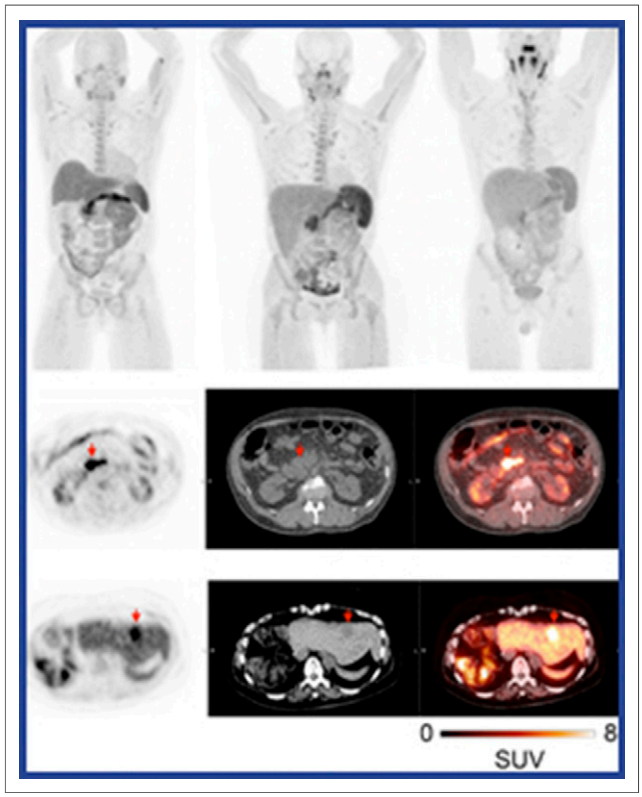

FIGURE 11. First-in-human images with ^{18}F-FluoroThanaTrace (^{18}F-TFT), a PARP-targeted PET tracer. Top row: PET images acquired at 30, 120, and 210 minutes after injection in 3 healthy volunteers. Middle row: ^{18}F-TFT PET, CT and fused transaxial images in a 52-year-old man with recurrent pancreatic cancer. Bottom row: transaxial PET, CT and fused images of a 62-year-old woman with metastatic biphenotypic hepatocellular carcinoma/cholangiocarcinoma.

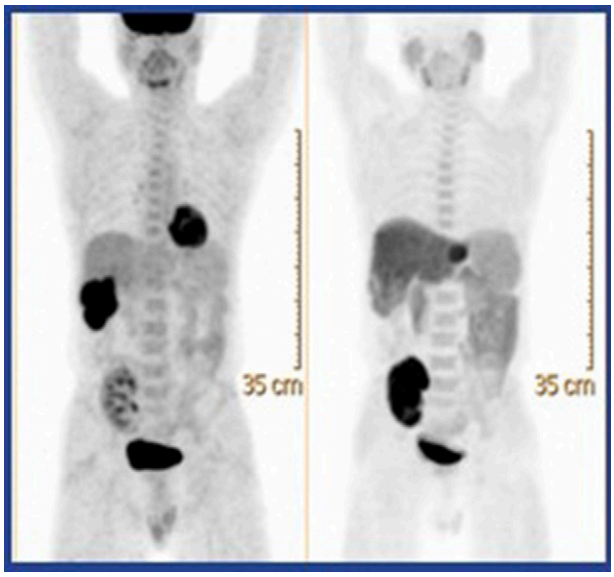

FIGURE 12. ^{18}F-FDG (left) and ^{18}F-FCH (right) PET images of a 63-year-old man with HBsAg (+) after renal transplantation with hepatocellular carcinomas in segment 6 and two-thirds of the liver. Individual lesions expressed variable FDG and FCH avidity.

It is also encouraging to see systematic phase III studies in progress with other radiopharmaceuticals. Kao et al. from the Buddhist Tzu-Chi Medical Foundation General Hospital (Hualien, Taiwan), Chung Shan Medical University Hospital (Taichung, Taiwan), E-Da Hospital (Kaohsiung, Taiwan), Kaohsiung Chang Gang Memorial Hospital (Taiwan), Lin Shin Hospital (Taichung, Taiwan), and National Taiwan University Hospital (Taipei) reported on "A phase III, multicenter, single-blind, cross-over study to evaluate the efficacy and safety of ^{18}F-fluorocholine comparing with ^{18}F-fluorodeoxyglucose for detecting hepatocellular carcinoma" [302]. The interesting finding of this study was that although both tracers accumulated in the hepatocellular carcinomas they also provided differential information. This is very nicely shown in the example in Figure 12, in a patient with 2 hepatomas. One is clearly FDG avid and the other is clearly FCH avid—so again it is not so much a question of which is better but of how can we combine the 2 tracers in an intelligent way in hepatocellular carcinoma imaging. These authors also observed in their conclusion that because hepatocellular lesions expressed variable FDG and FCH avidity, current histologic grading based on cell mitosis cannot adequately represent tumor metabolic change.

I would like to conclude with a nonradioisotope imaging approach. Although the majority of reports still focused on radioisotopes, we should remember that the name of our society is now the Society of Nuclear Medicine and Molecular Imaging, so it is welcome and important to note that we also received presentations about nonnuclear molecular imaging agents. Stoffels et al. from University Hospital Essen (Germany) and Thera Medical (München, Germany) reported on "Clinical application of noninvasive and nonradioactive determination of microscopic lymph node tumor status by multispectral optoacoustic imaging" [412]. This technology uses laser light to generate an ultrasound signal that is then detected by an ultrasound machine. Compared to optical imaging, the depth of penetration is significantly better. The other advantage is the combination of intrinsic contrast from blood and melanin and extrinsic contrast from near infrared–absorbing fluorescent dyes. This hybrid ultrasound/multispectral optoacoustic imaging combined with the near-infrared fluorophore indocyanine green (ICG) reliably visualized sentinel lymph nodes (SLNs) in vivo in 80 patients, with up to 5-cm penetration and 100% concordance with ^{99m}Tc-marked lymphoscintigraphy (Fig. 13). This technology has the potential not only to detect the sentinel node (based on the ICG) but also the metastatic melanoma cells based on the melanin signal.

Summary

A number of clear themes emerged at the SNMMI 2016 meeting. FDG was widely celebrated as the molecule of the century. Combined with PET/CT, FDG has redefined but (paradoxically) also narrowed the focus of clinical nuclear medicine over the last 15 years. However, we are now seeing the introduction of new imaging agents and therapeutic agents that are entering or likely to enter routine clinical use. This will broaden the scope of nuclear medicine practice and put more emphasis on therapy and the concept of theranostics. This is a very welcome change in our field and one that we should all embrace. Goethe said, "Everything ends if it does not change." The current rapid evolution in our field promises an exciting future of continued change and new discoveries that benefit a broad range of diseases and conditions.

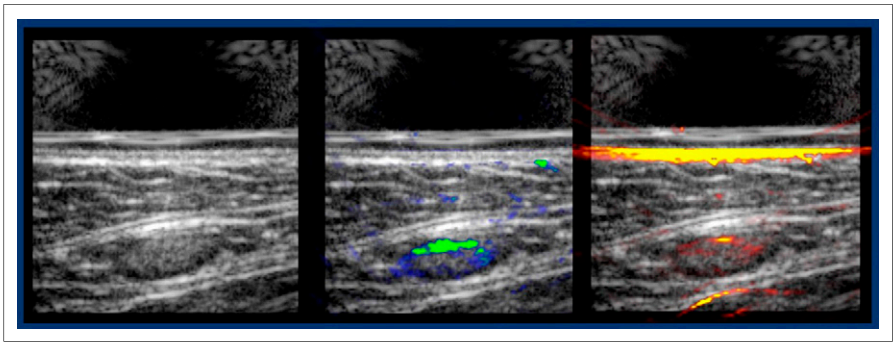

FIGURE 13. Ultrasound and multispectral optoacoustic imaging of a tumor-involved sentinel lymph node in a patient with melanoma. Left: B-mode ultrasound image of a lymph node. Middle: ICG signal superimposed on the ultrasound image, Right: melanin signal superimposed on the ultrasound image.